J|A|C|S
ARTICLES
Published on Web 01/27/2005

Detection of a Biomarker for Alzheimer's Disease from Synthetic and Clinical Samples Using a Nanoscale Optical Biosensor

Amanda J. Haes,[†,§] Lei Chang,[‡] William L. Klein,*[,‡] and Richard P. Van Duyne*[,†]

Contribution from the Department of Chemistry, Northwestern University, 2145 Sheridan Road, Evanston, Illinois 60208-3113, and Department of Neurobiology and Physiology, Northwestern University, 2205 Tech Drive, Evanston, Illinois 60208

Received September 28, 2004; E-mail: vanduyne@chem.northwestern.edu; wklein@northwestern.edu

Abstract: A nanoscale optical biosensor based on localized surface plasmon resonance (LSPR) spectroscopy has been developed to monitor the interaction between the antigen, amyloid-β derived diffusible ligands (ADDLs), and specific anti-ADDL antibodies. Using the sandwich assay format, this nanosensor provides quantitative binding information for both antigen and second antibody detection that permits the determination of ADDL concentration and offers the unique analysis of the aggregation mechanisms of this putative Alzheimer's disease pathogen at physiologically relevant monomer concentrations. Monitoring the LSPR-induced shifts from both ADDLs and a second polyclonal anti-ADDL antibody as a function of ADDL concentration reveals two ADDL epitopes that have binding constants to the specific anti-ADDL antibodies of 7.3×10^{12} M^{-1} and 9.5×10^{8} M^{-1}. The analysis of human brain extract and cerebrospinal fluid samples from control and Alzheimer's disease patients reveals that the LSPR nanosensor provides new information relevant to the understanding and possible diagnosis of Alzheimer's disease.

Introduction

The development of highly sensitive and selective biological sensors for the monitoring of disease biomarkers is an important motivation for nanoscience research. The localized surface plasmon resonance (LSPR) nanosensor has been demonstrated to be an effective platform for the quantitative detection of biological and chemical species.[1−8] The signal transduction mechanism of the LSPR nanosensor is based on its sensitivity to local refractive index changes near the surfaces of substrate-confined, size- and shape-controlled, silver and gold nanoparticles.[9−11] The LSPR of noble metal nanoparticles arises when electromagnetic radiation induces a collective oscillation of the conduction electrons of the individual nanoparticles[9,10,12−18] and has two primary consequences: (1) selective photon absorption which allows the optical properties of these nanoparticles to be monitored with UV−vis spectroscopy and (2) the enhancement of the electromagnetic fields surrounding the nanoparticles which is responsible for all surface-enhanced spectroscopies. The reader is referred to recent reviews[14,16,19−21] for a detailed description of the physics behind LSPR spectroscopy. The LSPR spectrum is measured by either transmission extinction spectroscopy[11,22] or dark-field light scattering spectroscopy.[23,24] The extinction spectra of the nanoparticles exhibit easily measured wavelength shifts that correspond to small changes in the refractive index within the electromagnetic fields surrounding the nanoparticles. It is well established that the extinction spectra of Ag and Au nanoparticles synthesized using nanosphere lithography (NSL) have refractive index sensitivities

[†] Department of Chemistry.
[‡] Department of Neurobiology and Physiology.
[§] Current address: Naval Research Laboratory, Washington D.C.

(1) Haes, A. J.; Hall, W. P.; Chang, L.; Klein, W. L.; Van Duyne, R. P. *Nano Lett.* **2004**, *4*, 1029.
(2) Haes, A. J.; Van Duyne, R. P. *J. Am. Chem. Soc.* **2002**, *124*, 10596.
(3) Haes, A. J.; Zou, S.; Schatz, G. C.; Van Duyne, R. P. *J. Phys. Chem. B* **2004**, *108*, 6961.
(4) Haes, A. J.; Zou, S.; Schatz, G. C.; Van Duyne, R. P. *J. Phys. Chem. B* **2004**, *108*, 109.
(5) Malinsky, M. D.; Kelly, K. L.; Schatz, G. C.; Van Duyne, R. P. *J. Am. Chem. Soc.* **2001**, *123*, 1471.
(6) Riboh, J. C.; Haes, A. J.; McFarland, A. D.; Yonzon, C. R.; Van Duyne, R. P. *J. Phys. Chem. B* **2003**, *107*, 1772.
(7) Englebienne, P. *Analyst* **1998**, *123*, 1599.
(8) Hirsch, L. R.; Jackson, J. B.; Lee, A.; Halas, N. J.; West, J. L. *Anal. Chem.* **2003**, *75*, 2377.
(9) El-Sayed, M. A. *Acc. Chem. Res.* **2001**, *34*, 257.
(10) Link, S.; El-Sayed, M. A. *J. Phys. Chem. B* **1999**, *103*, 8410.
(11) Haynes, C. L.; Haes, A. J.; Van Duyne, R. P. *Mater. Res. Soc. Symp. Proc.* **2001**, *635*, C6.3/1.
(12) Haynes, C. L.; Van Duyne, R. P. *J. Phys. Chem. B* **2001**, *105*, 5599.
(13) Mulvaney, P. *MRS Bull.* **2001**, *26*, 1009.
(14) Kreibig, U.; Gartz, M.; Hilger, A.; Hovel, H. Optical investigations of surfaces and interfaces of metal clusters. In *Advances in Metal and Semiconductor Clusters*; Duncan, M. A., Ed.; JAI Press Inc.: Stamford, CT, 1998; Vol. 4, p 345.
(15) Mulvaney, P. *Langmuir* **1996**, *12*, 788.
(16) Kreibig, U. Optics of nanosized metals. In *Handbook of Optical Properties*; Hummel, R. E., Wissmann, P., Eds.; CRC Press: Boca Raton, FL, 1997; Vol. II, p 145.
(17) Kreibig, U.; Gartz, M.; Hilger, A. *Ber. Bunsen-Ges.* **1997**, *101*, 1593.
(18) Jensen, T. R.; Kelly, K. L.; Lazarides, A.; Schatz, G. C. *J. Cluster Sci.* **1999**, *10*, 295.
(19) Schatz, G. C.; Van Duyne, R. P. *Electromagnetic Mechanism of Surface-Enhanced Spectroscopy*; Wiley: New York, 2002; Vol. 1.
(20) Haes, A. J.; Van Duyne, R. P. *Expert Review of Molecular Diagnostics* **2004**, *4*, 527.
(21) Haes, A. J.; Stuart, D. A.; Nie, S.; Van Duyne, R. P. *J. Fluoresc.* **2004**, *14*, 355.
(22) Jensen, T. R.; Malinsky, M. D.; Haynes, C. L.; Van Duyne, R. P. *J. Phys. Chem. B* **2000**, *104*, 10549.
(23) Van Duyne, R. P.; Haes, A. J.; McFarland, A. D. *SPIE* **2003**, *5223*, 197.
(24) McFarland, A. D.; Van Duyne, R. P. *Nano Lett.* **2003**, *3*, 1057.

10.1021/ja044087q CCC: $30.25

of ~200 nm/RIU[3,5] and a sensing volume that can be tuned by controlling nanoparticle size, shape, and composition.[3,4]

The need for ultrasensitive detection methods for biological and chemical sample screening is an important issue in disease diagnosis and mechanistic understanding. For example, Alzheimer's disease (AD), a progressive neurodegenerative disease for which there is neither a cure nor a good clinical diagnostic, is the leading cause of dementia in people over age 65 and affects over four million Americans. Genetic, biochemical, and animal model studies strongly suggest a central role for amyloid-β (Aβ) in the pathogenesis of AD.[25] Aβ is a 42-amino acid peptide that was first discovered as the monomeric subunit of the large insoluble amyloid fibrils of AD plaques. In the past several years, it has been found that, in addition to plaques, Aβ will also self-assemble into small soluble oligomers, termed ADDLs, (amyloid-derived diffusible ligands), and that ADDLs will cause neurological dysfunctions relevant to memory.[26−28] Two comprehensive reviews of current data have concluded that early stages of the disease are likely to be caused by the synaptic impact of such soluble oligomeric assemblies of Aβ.[29,30] Despite the fact that several molecules including Aβ_{1-40}, Aβ_{1-42}, tau, phosphorylated tau, and seeded Aβ forms or their combination have been suggested as potential AD biomarkers,[31−33] at the present time, there is no definite clinical diagnosis for AD other than autopsy. Recently, it has been demonstrated that ADDLs are present at significantly elevated levels in autopsied brain samples from humans with AD.[34] The association of ADDLs with disease mechanisms and brain pathology suggests that a sensitive means to detect ADDLs in body fluid could provide a definitive molecular basis for the laboratory diagnosis of AD. An ultrasensitive method for ADDLs detection potentially could emerge from LSPR nanosensor technology, providing an opportunity to develop the first clinical lab diagnostic for AD.

In this study, we combine LSPR nanosensor technology with Aβ oligomer specific antibodies to determine if ADDLs are a potential biomarker for AD. In comparison with other biosensing approaches, the LSPR nanosensor allows for the analysis of biological species in a surfactant-free environment. This is extremely important because the absence of a surfactant allows for biological species to be analyzed in their native state (not one influenced by the presence of physiologically unnatural molecules). In addition, the LSPR nanosensor is demonstrated to be sufficiently sensitive for the detection of ultralow concentrations of ADDLs in biological samples. By optimizing the size of the nanoparticles, the sensing distance of the nanoparticles extends ~35 nm from the surface. This sensing distance is required for the implementation of a sandwich assay for the target ADDL molecules. Quantitative detection models for both the ADDL and the second anti-ADDL antibody response are developed to extract information regarding the affinity constants between the antigen and antibody species and to aid in the analysis of human samples. Human brain extracts and cerebrospinal fluid (CSF) samples from control and diseased patients exhibit drastically different responses, which indicate the presence of elevated ADDL concentrations in the samples from diseased patients in comparison to the control patients. These preliminary results indicate that LSPR nanosensor technology is useful as a screening method of human samples for disease diagnosis as well as a more general approach to a mechanistic understanding of diseases and drug target interactions.

Methods and Materials

Materials. 11-Mercaptoundecanoic acid (11-MUA) and 1-octanethiol (1-OT) were purchased from Aldrich (Milwaukee, WI). Phosphate-buffered saline (PBS) solutions of 10 and 20 mM, pH 7.4, was purchased from Sigma (St. Louis, MO). 1-Ethyl-3-[3-dimethy-laminopropyl]carbodiimide hydrochloride (EDC) was obtained from Pierce (Rockford, IL). Absolute ethanol was obtained from Pharmco (Brookfield, CT). Methanol was purchased from Fisher Scientific (Pittsburgh, PA). Silver wire (99.99%, 0.5-mm diameter) was purchased from D. F. Goldsmith (Evanston, IL). Tungsten vapor deposition boats and chromium rods were acquired from R. D. Mathis (Long Beach, CA). Polystyrene spheres of 390 nm ± 19.5 nm were received as a suspension in water from Duke Scientific (Palo Alto, CA). Millipore cartridges (Marlborough, MA) were used to purify water to a resistivity of 18.2 MΩ cm^{-1}. Triton X-100 was purchased from Aldrich (Milwaukee, WI). Ruby red muscovite mica substrates were purchased from Asheville-Schoonmaker Mica Co. (Newport News, VA).

Synthetic ADDL and Anti-ADDL Antibody Preparation. Aβ_{1-42} peptide (California Peptide Research, Napa, CA) was used to prepare synthetic ADDLs according to published protocols.[26] An aliquot of Aβ_{1-42} was dissolved in anhydrous DMSO to a concentration of 22.5 mg/mL (5 mM), pipet mixed, and further diluted into ice-cold F12 medium (phenol red free) (BioSource, CA) at a ratio of 1:50. The mixture was quickly vortexed, incubated at 6−8 °C for 24 h, and centrifuged at 14 000*g* for 10 min. The oligomers were then collected from the supernatant. The concentration of synthetic ADDLs was determined by a micro-BCA assay (Pierce, Rockford, IL). A similar protocol was followed for vehicle preparation except no Aβ peptide was added. Antibodies targeting ADDLs in the LSPR immunoassay (polyclonal M71 and monoclonal 20C2) were generated and characterized as previously described.[35]

CSF and Brain Extract Preparation. CSF samples were provided by Dr. John Lee, Loyola University Medical School, Maywood, IL. Premortem samples were obtained via lumbar puncture and kept frozen until used. Tissues of cortex of AD (pathology diagnosis based on Braak & Braak, CERAD, and NIA/Reagan Institute Criteria) and age-matched control brains were obtained from Northwestern University Alzheimer's Brain Bank and stored at −80 °C before using. Brain extracts were prepared following the literature.[34] One hundred milligrams of tissue was homogenized in 1 mL Ham's F12 medium (phenol-free BioSource, Camarillo, CA) containing protease inhibitors (complete mini-EDTA free tablet, Roche, Indianapolis, IN) on ice using A Tissue Tearor (Biospec Products, Bartlesville, OK). After centrifugation at 20 000*g* for 10 min, the supernatant was centrifuged at 100 000*g* for 60 min.

(25) Selkoe, D. J.; Hardy, J. *Science* **2002**, *298*, 963.
(26) Lambert, M. P.; Barlow, A. K.; Chromy, B. A.; Edwards, C.; Freed, R.; Liosatos, M.; Morgan, T. E.; Rozovsky, I.; Trommer, B.; Viola, K. L.; Wals, P.; Zhang, C.; Finch, C. E.; Krafft, G. A.; Klein, W. L. *Proc. Natl. Acad. Sci. U.S.A.* **1998**, *95*, 6448.
(27) Walsh, D. M.; Klyubin, I.; Fadeeva, J. V.; Cullen, W. K.; Anwyl, R.; Wolfe, M. S.; Rowan, M. J.; Selkoe, D. J. *Nature* **2002**, *416*, 535.
(28) Chromy, B. A.; Nowak, R. J.; Lambert, M. P.; Viola, K. L.; Chang, L.; Velasco, P. T.; Jones, B. W.; Fernandez, S. J.; Lacor, P. N.; Horowitz, P.; Finch, C. E.; Krafft, G. A.; Klein, W. L. *Biochemistry* **2003**, *42*, 12749.
(29) Mattson, M. P. *Nature* **2004**, *430*, 631.
(30) Hardy, J.; Selkoe, D. J. *Science* **2002**, *297*, 353.
(31) Hampel, H.; Mitchell, A.; Blennow, K.; Frank, R. A.; Brettschneider, S.; Weller, L.; Moller, H. J. *J. Neural Transmission* **2004**, *111*, 247.
(32) Pitschke, M.; Prior, R.; Haupt, M.; Riesner, D. *Nature Medicine* **1998**, *4*, 832.
(33) Seubert, P.; Vigopelfrey, C.; Esch, F.; Lee, M.; Dovey, H.; Davis, D.; Sinha, S.; Schlossmacher, M.; Whaley, J.; Swindlehurst, C.; McCormack, R.; Wolfert, R.; Selkoe, D.; Lieberburg, I.; Schenk, D. *Nature* **1992**, *359*, 325.
(34) Gong, Y.; Chang, L.; Viola, K. L.; Lacor, P. N.; Lambert, M. P.; Finch, C. E.; Krafft, G. A.; Klein, W. L. *Proc. Natl. Acad. Sci. U.S.A.* **2003**, *100*, 10417.
(35) Lambert, M. P.; Viola, K. L.; Chromy, B. A.; Chang, L.; Morgan, T. E.; Yu, J. X.; Venton, D. L.; Krafft, G. A.; Finch, C. E.; Klein, W. L. *J. Neurochem.* **2001**, *79*, 595.

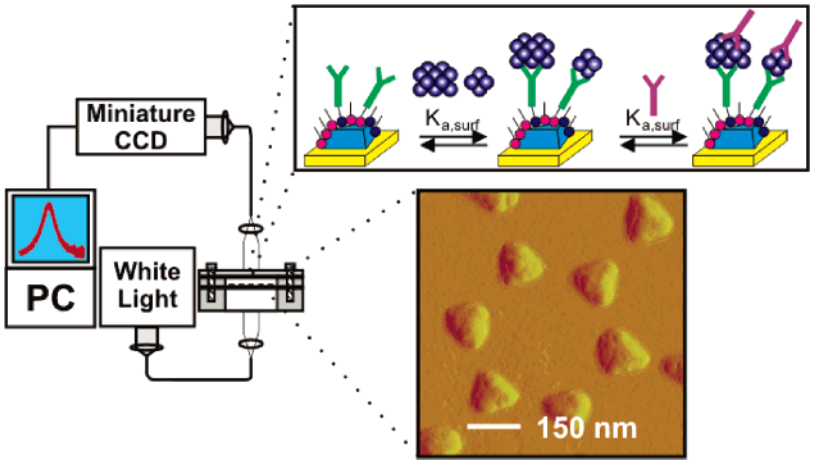

Figure 1. Design and experimental setup for the LSPR biosensor for the detection of ADDLs using a sandwich assay. Transmission UV−vis spectroscopy is used to monitor the optical properties (LSPR) of Ag nanoparticles. The schematic illustration displays the sandwich assay and surface chemistry of the LSPR nanosensor. First, surface-confined Ag nanoparticles (see AFM inset, nanoparticle width = 90 nm, nanoparticle height = 25.0 nm) are synthesized using NSL on mica substrates. Next, a SAM layer consisting of a mixed monolayer of OT and MUA passivates the nanoparticles for nonspecific binding and activates the nanoparticles for the attachment of the first anti-ADDL antibody, respectively. The first anti-ADDL antibody is covalently attached to the nanoparticles via incubation in 100 mM EDC/100 nM anti-ADDL antibody solution for 1 h. Samples are then incubated in varying concentrations of ADDLs for 30 min. Finally, to enhance the LSPR shift response of the ADDLs, the samples are incubated in a 100 nM anti-ADDL solution for an additional 30 min.

Protein concentration of 100 000*g* supernatant was determined by standard BCA assay. Fractions were stored at −80 °C. Gloves were worn at all times when handling all biological materials.

Nanoparticle Fabrication. Nanosphere lithography (NSL) was used to create monodisperse, surface-confined Ag nanotriangles.[2,4] Polystyrene nanospheres (diameter = 390 nm + 19.5 nm, Duke Scientific) were diluted as a 1:1 solution with Triton X-100 and methanol (1:400 by volume). Approximately 4 μL of this solution was drop-coated onto the freshly cleaved mica substrates[2] and allowed to dry, forming a monolayer in a close-packed hexagonal formation, which served as a deposition mask. The samples were mounted into a Consolidated Vacuum Corporation vapor-deposition chamber. A Leybold Inficon XTM/2 quartz crystal microbalance was used to monitor the thickness of the metal being deposited. For all experiments, 25 nm of Ag (D. F. Goldsmith) was evaporated onto the samples. Following metal deposition, the samples were sonicated for 3−5 min in ethanol (Pharmco) to remove the polystyrene nanosphere mask, creating Ag triangular nanoparticles on the mica substrate.

Ultraviolet−Visible Extinction Spectroscopy. Macroscale UV−vis extinction measurements were collected using an Ocean Optics (Dunedin, FL) S2000 fiber optically coupled spectrometer with a CCD detector. All spectra in this study are macroscopic measurements performed in standard transmission geometry with unpolarized light. The probe diameter was approximately 1 mm. A home-built flow cell[5] was used to control the external environment of the Ag nanoparticle substrates.

Nanoparticle Functionalization. Immediately following nanosphere removal, the samples were incubated for 24−48 h in 3:1 1 mM 1-OT/1 mM 11-MUA solution (in ethanol). Next, the samples were rinsed thoroughly with ethanol and dried with N_2. Following SAM functionalization, the samples were incubated in a 100 nM anti-ADDL antibody solution in 10 mM PBS. Covalent linking was ensured via the presence of 100 mM EDC during this 1-h incubation period. Exposing the sample to varying concentrations of ADDL in 10 mM PBS for 30 min was the first detection step of the immunoassay. The assay was completed via the incubation of the sample in 100 nM anti-ADDL antibody in 10 mM PBS for 30 min. Experiments were performed using a monoclonal antibody for the second antibody; however, no notable differences were observed in the LSPR shift response data. For this reason, only polyclonal antibodies were used for these sandwich assays.

Nonspecific interactions were monitored by exposing the SAM functionalized nanoparticles to a 250 nM anti-ADDL antibody solution (no EDC coupling agent) for 1 h. For the sandwich assay experiments involving the human samples, following SAM modification, the samples were incubated in a 100 nM anti-ADDL/100 mM EDC solution in 10 mM PBS for 1 h. Next, the sample was exposed to varying concentrations of human brain extract or CSF for 30 min. Finally, the sample was exposed to 100 nM ADDL solution for 30 min. Samples were rinsed with cycles of 10 mM PBS and 20 mM PBS (with 0.1% Tween 20) following each functionalization step to ensure the removal of nonspecifically bound species. For the binding curves in Figure 4A and 4B, each data point represents averaged experimental results from a minimum of two fresh samples.

Atomic Force Microscopy. Atomic force microscope (AFM) images were collected using a Digital Instruments Nanoscope IV microscope and Nanoscope IIIa controller operating in tapping mode. The resulting AFM linescan analysis reveal that the bare triangular nanoparticles have ∼90-nm perpendicular bisectors and ∼25-nm heights.

Results

Detection of ADDLs Using an Antibody Sandwich Assay. For the first time, a sandwich assay has been accomplished using the LSPR nanosensor technology. Figure 1A shows a schematic representation of the nanoparticle structure and chemical functionalization for the sandwich assay. Briefly, triangular Ag nanoparticles (perpendicular bisectors = 90 nm, heights = 25 nm) are synthesized on mica substrates and functionalized with antibodies specific for ADDLs. Next, the nanoparticle surface is exposed to varying concentrations of synthetic ADDLs. Finally, the nanosensor is exposed to a fixed concentration of anti-ADDL antibody for 30 min to complete the assay. A polyclonal anti-ADDL antibody was used in both instances of antibody exposure.

By functionalizing the Ag nanoparticles with a self-assembled monolayer (SAM), the stability of the samples is greatly increased and consistent red shifts[2] are produced upon incubation in given concentrations of ADDLs and the second anti-ADDL antibody. Because it is hypothesized that the formation ADDLs may be implicated in the early symptoms associated with AD, an assay that targets these molecules at sub-nanomolar concentrations is desired. A sandwich assay that relies on the specific interactions between ADDLs and their antibodies is the most

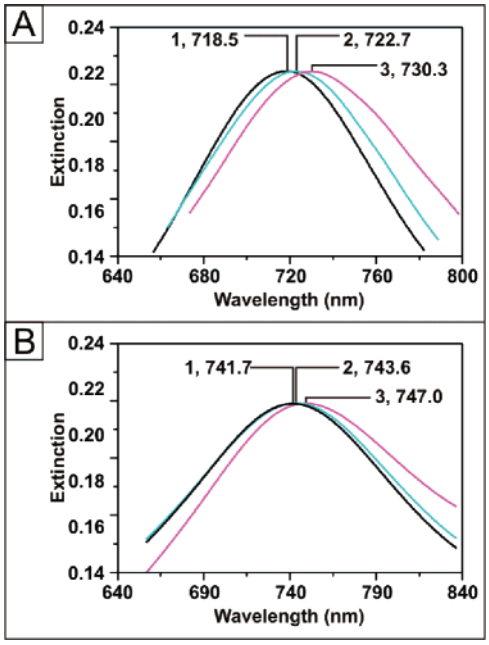

Figure 2. Demonstration of the LSPR sandwich assay at high and low concentrations. (A) LSPR spectra for each step of the sandwich assay for 10 pM ADDL. Ag nanoparticles after modification with (A-1) 100 nM anti-ADDL antibody, $\lambda_{max} = 718.5$ nm, (A-2) 10 pM ADDL, $\lambda_{max} = 722.7$ nm, and (A-3) 100 nM anti-ADDL, $\lambda_{max} = 730.3$ nm. (B) LSPR spectra for each step of the sandwich assay for 100 fM ADDL. Ag nanoparticles after modification with (B-1) 100 nM anti-ADDL antibody, $\lambda_{max} = 741.7$ nm, (B-2) 100 fM ADDL, $\lambda_{max} = 743.6$ nm, and (B-3) 100 nM anti-ADDL, $\lambda_{max} = 747.0$ nm. All spectra were collected in N_2.

straightforward method to analyze and detect these molecules. To perform this sandwich assay, implementation of the optimization of nanoparticle size and sensing distances were employed.[4] That is, the nanoparticles were fabricated to have electromagnetic fields or an effective sensing distance that extends ~35 nm away from their surface.[4]

Representative sandwich assays for the direct detection of high and low concentrations of ADDLs are displayed in Figure 2. In this study, anti-ADDL antibody was specifically linked to the SAM functionalized nanoparticles over a 1-h period. Next, the nanosensor is exposed to a 10 pM ADDL (Figure 2A) solution for 30 min. During the ADDL incubation, the extinction maximum of the sample shifts from 718.5 nm (Figure 2A-1) to 722.7 nm (Figure 2A-2), a 4.2-nm shift. Next, this shift is amplified by exposing the sample to an additional anti-ADDL antibody for 30 min resulting in an additional 7.6-nm wavelength shift or a total LSPR shift of 11.8 nm. When this sandwich assay is repeated with 100 fM ADDL (Figure 2B), the LSPR extinction maximum shifts 1.9 nm (from 741.7 to 743.6 nm) upon exposure to ADDLs. An additional 3.4-nm shift is observed upon incubation in the second antibody for a total LSPR shift of 5.3 nm. The samples were checked for nonspecific binding after step 1, and no nonspecific binding was observed.

Elimination of Nonspecific Binding Using Mica Substrates. The development of a successful sensor protocol requires the demonstration of minimal to no nonspecific binding. In our previous studies for implementing the LSPR nanosensor technology with an immunoassay specific for targeting antibodies of AD markers,[1] the LSPR nanosensor response was dominated by nonspecific interactions at low target molecule concentrations. The source of this undesirable response was attributed to

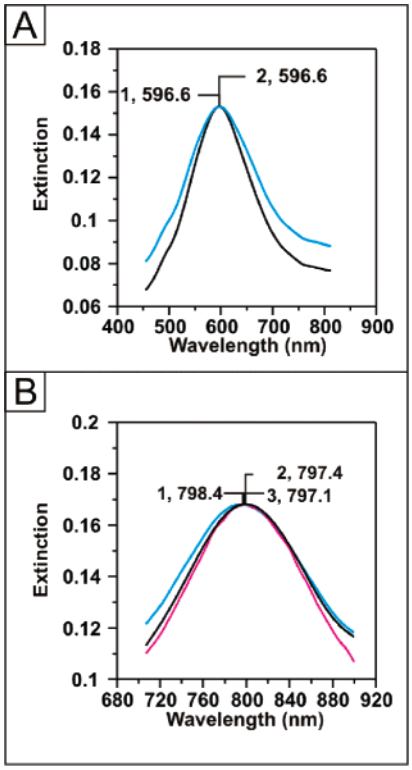

Figure 3. LSPR spectra illustrating the lack of nonspecific binding for the LSPR nanosensor. (A) Demonstration of nonspecific binding elimination from anti-ADDL antibody to SAM-functionalized nanoparticles on mica. (A-1) Ag nanoparticles after modification with 1:3 1 mM 11-MUA:1-OT, $\lambda_{max} = 596.6$ nm, and (A-2) Ag nanoparticles after exposure to 250 nM anti-ADDLs (in the absence of EDC), $\lambda_{max} = 596.6$ nm. (B) Demonstration of the absence of nonspecific binding from a vehicle solution to anti-ADDL antibody functionalized nanoparticles on mica. Ag nanoparticles after modification with (B-1) 100 nM anti-ADDL antibody, $\lambda_{max} = 798.4$ nm, (B-2) vehicle, $\lambda_{max} = 797.4$ nm, and (B-3) 100 nM anti-ADDL, $\lambda_{max} = 797.1$ nm. All spectra were collected in a N_2 environment.

a molecular interaction with the Cr adhesion layer. While silane passivation decreased this undesirable result, it did not totally eliminate the problem. Presently, we have made great strides to overcome the nonspecific binding observed with the Cr containing nanoparticles. First, mica substrates have been substituted in place of the glass substrates and the use of Cr as an adhesion layer has been eliminated. The adhesion of silver to mica is sufficiently great that the nanoparticles remain surface-bound throughout an experiment.[6] Additionally, as seen in Figure 3A, when a SAM functionalized nanoparticle surface is exposed to 250 nM anti-ADDL solution for an hour without the use of a coupling agent (EDC), no shift in the LSPR wavelength is observed. This indicates that no antibody is randomly attaching to the nanoparticle sample and that the nonspecific interactions that had previously plagued the LSPR nanosensor shift responses have been eliminated.

A second nonspecific binding experiment is performed to analyze the influence of the biological vehicle (see Materials and Methods for description) on the LSPR response of an antibody functionalized nanoparticle sample (Figure 3B). To test for this nonspecific interaction, the LSPR nanosensor is first specifically functionalized with anti-ADDL antibodies using an EDC coupling agent ($\lambda_{max} = 798.4$ nm, Figure 3B-1). Next, the sensor surface was exposed to the biological vehicle for 30 min revealing a slight blue-shift to 797.4 nm, Figure 3B-2. Finally, the sensor surface was exposed to 100 nM anti-ADDL

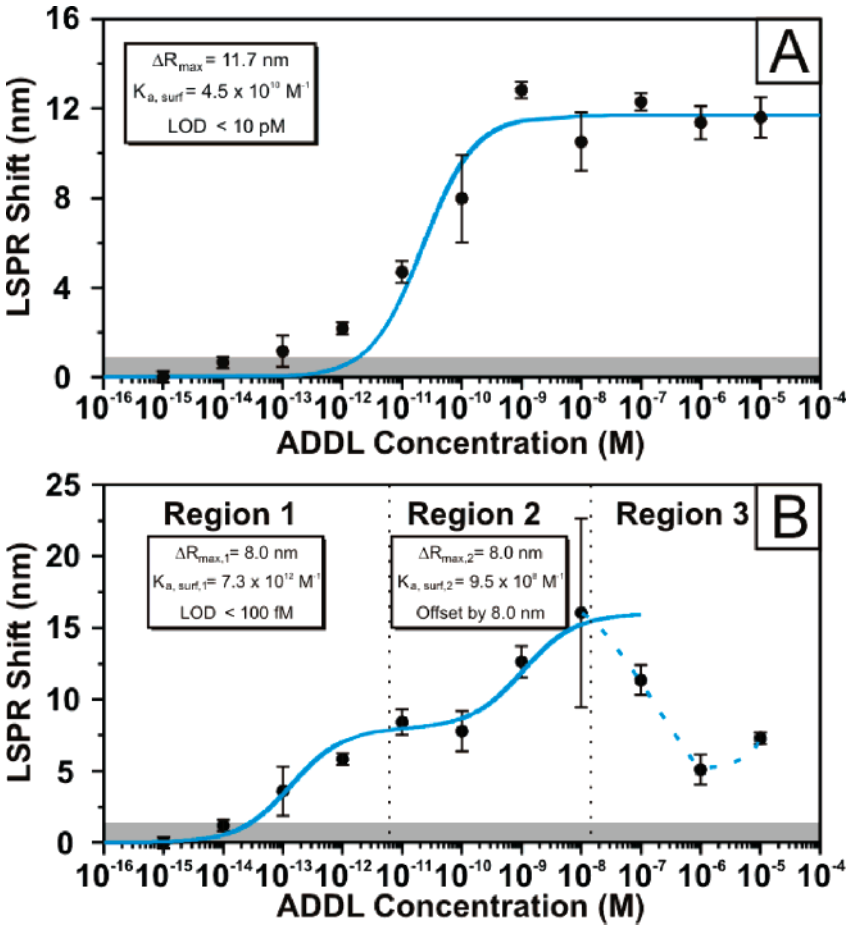

Figure 4. Quantitative response curves. (A) LSPR shift, ΔR or $\Delta\lambda_{max}$, versus [ADDL] response curve for the binding of ADDLs to an anti-ADDL antibody functionalized Ag nanobiosensor. All measurements were collected in a N_2 environment. The solid line is the calculated value of ΔR using eq 1. The shaded box indicates the limit of detection as determined from the spectrometer noise (3 times the smallest reliable wavelength shift measured). Error bars represent the spread in the data. (B) Enhanced LSPR shift, ΔR or $\Delta\lambda_{max}$, versus [anti-ADDL antibody] response curve for the binding of second anti-ADDL antibody to the ADDL functionalized Ag nanobiosensor. All measurements were collected in a N_2 environment. The solid line is the calculated value of ΔR using eq 2. The shaded box indicates the limit of detection as determined from the spectrometer (3 times the smallest reliable wavelength shift measured). Error bars represent the spread in the data. The data are divided into three detection regions: (region 1) response for concentrations less than 10 pM, (region 2) response for concentrations between 10 pM through 10 nM, and (region 3) response for concentrations greater than 10 nM.

antibody for an additional 30 min. Once again, a slight blue-shift in the LSPR extinction maximum to 797.1 nm (Figure 3B-3) is observed. These small blue-shifts, which indicate that no additional mass is being detected at the nanoparticle sensor chip, can be attributed either to the removal of a small amount of covalently bound anti-ADDL antibody from the substrate or to slight variations in spectrometer noise. Considering nonspecific binding and the peak-to-peak wavelength shift noise of the baseline in repetitive experiments (~0.3 nm), one can conservatively estimate the smallest, reliable LSPR wavelength shift as 3 times this value (~0.9 nm).

Quantification of ADDL and Second Anti-ADDL Antibody Response. To thoroughly investigate the influence of varying concentrations of ADDLs on the LSPR nanosensor response, the shift induced by the direct binding of ADDLs onto the anti-ADDL antibody functionalized nanoparticle surface has been analyzed. To develop a more quantitative understanding of the concentration-dependent response, only the shift from the ADDLs and not the response from the second antibody is included. The LSPR λ_{max} shift, $\Delta\lambda_{max} = \Delta R$, versus [ADDL] response curve was measured over the concentration range 1 fM < [ADDL] < 10 μM (Figure 4A). While the thermodynamic affinity constant between antibodies and their specific antigens is by no means large enough to be considered irreversible, sample incubation and rinsing conditions have been optimized to minimize nonspecific interactions while retaining the largest possible LSPR shift response.

Figure 4A shows the experimental data for the ADDL shifts plotted as the LSPR λ_{max} shift, ΔR versus [ADDL]. The experimental response curve for ADDLs has been quantitatively interpreted in terms of a model that makes the following assumptions: (1) 1:1 binding of a solution-phase multivalent analyte (ADDL) with different sites but invariant affinities to the surface-bound capture ligand (anti-ADDL antibody); (2) the only operative nanoparticle sensing mechanism is the change in the local refractive index caused by the adsorbed analyte (ADDL); and (3) the measured LSPR λ_{max} shift response, ΔR, is proportional to the thickness (and mass) of the adsorbed analyte layer and its refractive index. The response curve can be described by the following equation:[6]

$$\Delta R = \Delta R_{max}\left[\frac{K_{a,surf}[ADDL]}{1 + K_{a,surf}[ADDL]}\right] \quad (1)$$

where $\Delta R = \Delta\lambda_{max}$, LSPR λ_{max} shift for a given concentration, ΔR_{max} is the maximum LSPR response at high concentrations,

$K_{a,surf}$ is the surface-confined thermodynamic affinity constant, and [ADDL] is the concentration of the ADDL solution.

Comparing the experimentally measured ΔR versus [ADDL] response (points) to eq 1 (solid line, Figure 4A) yields approximate values for $\Delta R_{max} = 11.7$ nm and a surface-confined thermodynamic affinity constant $K_{a,surf} = 4.5 \times 10^{10}$ M^{-1}. In addition, the data in Figure 4A allows one to estimate the limit of detection (LOD) for the LSPR nanobiosensor for ADDL detection separate from the enhanced shift from the second anti-ADDL antibody. The peak-to-peak wavelength shift noise of the baseline in repetitive experiments is ~0.3 nm. Taking the limit of detection as 3 times this value, one conservatively estimates a LOD of ~10 pM.

Figure 4B displays the experimental data for the second anti-ADDL antibody shift response plotted as the LSPR λ_{max}, ΔR versus [ADDL]. As a reminder, a fixed (100 nM) second anti-ADDL antibody concentration was exposed to the LSPR nanosensor substrates that had been exposed to varying ADDL concentrations. These data are not accurately described by the previous binding model. Instead, the experimental response curve has been quantitatively predicted in terms of a model that makes the following assumptions: (1) multiple (two) receptors of solution phase multivalent analytes (anti-ADDL antibody) with different sites but invariant affinities to the surface-bound capture ligands (ADDL); (2) the only operative nanoparticle sensing mechanism is the change in the local refractive index caused by the adsorbed analyte (anti-ADDL antibody); and (3) the measured LSPR λ_{max} shift response, ΔR, is determined only by the thickness of the adsorbed analyte layer and its refractive index. The response curve can be described by the following equation:[6]

$$\Delta R = \Delta R_{max,1}\left[\frac{K_{a,surf,1}[ADDL]}{1 + K_{a,surf,1}[ADDL]}\right] + \Delta R_{max,2}\left[\frac{K_{a,surf,2}[ADDL]}{1 + K_{a,surf,2}[ADDL]}\right] \quad (2)$$

where $\Delta R = \Delta\lambda_{max}$, LSPR λ_{max} shift induced by the second anti-ADDL antibody for a given ADDL concentration, $\Delta R_{max,1}$ is the maximum LSPR response at concentrations in region 1, $\Delta R_{max,2}$ is the added LSPR shift response above $\Delta R_{max,1}$ at concentrations in region 2, $K_{a,surf,1}$ is the surface-confined thermodynamic affinity constant in region 1, $K_{a,surf,2}$ is the surface-confined thermodynamic affinity constant in region 2, and [ADDL] is the concentration of ADDLs in solution.

This model accurately predicts the second anti-ADDL antibody response for ADDL concentrations ranging from 1 fM to 100 nM. As displayed in Figure 4B, three binding regimes are revealed. Region 1, which covers ADDL concentrations below 10 pM, reveals an extremely strong antigen/antibody interaction with a binding constant ($K_{a,surf,1}$) of 7.3×10^{12} M^{-1} and a limit of detection (LOD) <100 fM. Region 2, which covers ADDL concentrations between 10 pM to 100 nM, describes an average antigen/antibody interaction with a binding constant ($K_{a,surf,2}$) of 9.5×10^{8} M^{-1}. At concentrations greater than 100 nM (region 3), the second anti-ADDL antibody response begins to deviate from the binding model. While the quantitation of ADDLs at these concentrations is biologically irrelevant, we have included these data for completeness. The origin of the observed decrease in response at high ADDL concentrations is under investigation.

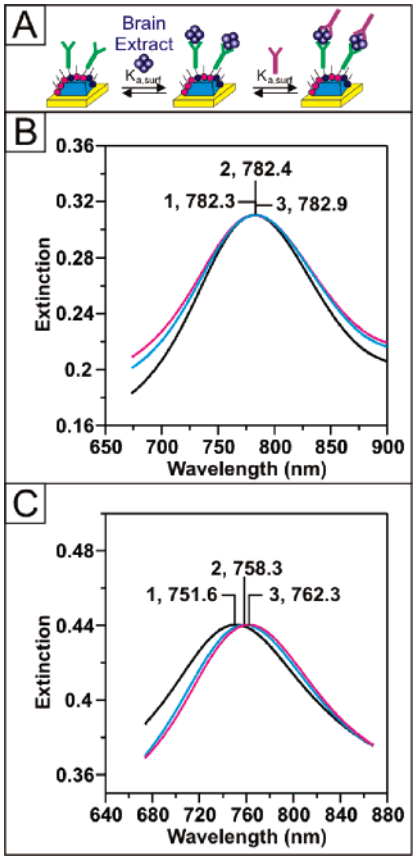

Figure 5. Analysis of human brain extract samples using a sandwich assay and the LSPR nanosensor. (A) Surface chemistry for the possible ADDL detection in human brain extract samples using the antibody sandwich assay. (B) Control patient: LSPR spectra for each step of the assay. Ag nanoparticles after functionalization with (B-1) 100 nM anti-ADDL (100 mM EDC) (λ_{max} = 782.3 nm), (B-2) control brain extract (λ_{max} = 782.4 nm), and (B-3) 100 nM anti-ADDL (λ_{max} = 782.9 nm). (C) AD patient: LSPR spectra for each step of the assay. Ag nanoparticles after functionalization with (C-1) 100 nM anti-ADDL (100 mM EDC) (λ_{max} = 751.6 nm), (C-2) diseased brain extract (λ_{max}=758.3 nm), and (C-3) 100 nM anti-ADDL (λ_{max} = 762.3 nm). All measurements were collected in N_2.

Alzheimer's Disease Assay Using Human Samples. To date, the only systems probed with the LSPR nanosensor have been model systems such as biotin/streptavidin[2] and biotin/antibiotin.[6] Because of our encouraging nonspecific binding results and the quantitative models revealed in the standard sandwich assay described above, it was decided that two types of human samples would be attempted: human brain extract and cerebrospinal fluid. In both cases, duplicate samples from a control and an AD patient were analyzed. These initial data suggest promising results for clinical sample analysis using LSPR nanosensor technology.

In the first comparison, human brain extract was prepared and exposed to an anti-ADDL antibody functionalized LSPR nanosensor chip for 30 min. After thorough rinsing, the sample's response was enhanced via exposure to a second anti-ADDL antibody (Figure 5). The assays were performed in duplicate. Figure 5B reveals a representative assay from an age-matched brain extract sample. During the brain extract incubation, the extinction maximum of the sample shifted from 782.3 nm (Figure 5B-1) to 782.4 nm (Figure 5B-2), a 0.1-nm shift. Next, this shift was amplified by exposing the sample to an additional

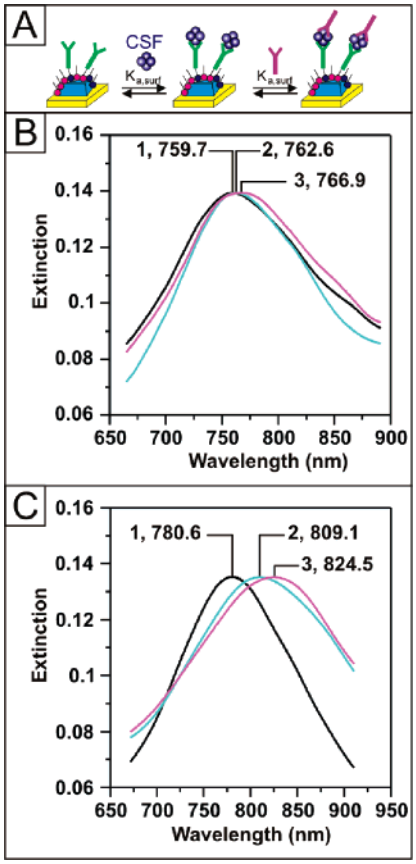

Figure 6. Analysis of human CSF samples using a sandwich assay and the LSPR nanosensor. (A) Surface chemistry for the possible ADDL detection in human CSF samples using the antibody "sandwich" assay. (B) Aging patient: LSPR spectra for each step of the assay. Ag nanoparticles after functionalization with (B-1) 100 nM anti-ADDL (100 mM EDC) (λ_{max} = 759.7 nm), (B-2) CSF (λ_{max} = 762.6 nm), and (B-3) 100 nM anti-ADDL (λ_{max} = 766.9 nm). (C) AD patient: LSPR spectra for each step of the assay. Ag nanoparticles after functionalization with (C-1) 100 nM anti-ADDL (100 mM EDC) (λ_{max} = 780.6 nm), (C-2) CSF (λ_{max} = 809.1 nm), and (C-3) 100 nM anti-ADDL (λ_{max} = 824.5 nm). All measurements were collected in a N_2 environment.

anti-ADDL antibody for 30 min resulting in an additional 0.5-nm wavelength shift or a total LSPR shift of 0.6 nm. This response is below the reliable detection capabilities of the LSPR nanosensor sandwich assay as predicted from the quantitative analysis in Figure 4A and 4B. Additionally, this small response indicates that the LSPR nanosensor can be used for human sample analysis without undue concern for nonspecific binding.

Analysis of the AD sample reveals completely different behavior. A representative assay is shown in Figure 5C. Upon incubation of the antibody functionalized sensor substrate in the diseased brain extract, the LSPR extinction maximum shifts from 751.6 nm (Figure 5C-1) to 758.3 nm (Figure 5C-2) giving an LSPR shift of 6.7 nm. This response is amplified by an additional 4.0 nm by the second anti-ADDL antibody revealing an easily detected total shift of 10.7 nm.

While detection of ADDL in brain extract is encouraging, this assay can only be completed postmortem. Ideally, one would perform this assay in a body fluid that can be extracted while a person is still alive. For that reason, the LSPR sandwich assay was used to analyze cerebrospinal fluid (CSF) from a control and AD patient. Preliminary results indicate a large difference between aging and AD patient samples. As seen in Figure 6A, a small 2.9-nm LSPR shift was observed after exposing the CSF sample from an aging patient onto the antibody functionalized substrate. This shift was amplified by 4.3 nm with the second anti-ADDL antibody. The results in Figure 6B are dramatically different. When this antibody functionalized sample is exposed to a CSF sample from a patient with AD, an 18.5-nm shift is observed. This shift is magnified by an additional 15.4 nm after exposure to the second antibody resulting in a total shift of 33.9 nm.

Discussion

To date, much of nanoscience research has been focused on understanding the fundamental science involved rather than on the implementation of successful applications for biological or chemical analysis. As demonstrated in this work, the potential of nanoscale optical biosensors when combined with specific and novel biological materials are far reaching and will aid in the development of other successful nanotechnology-based devices. The development of nanodevices, including nanosensors that are highly sensitive and selective (give low false positives, low false negatives), will provide a major improvement over current technologies for disease understanding, treatment, and monitoring. Instruments that provide high throughput screening for drug discovery and disease diagnosis will uncover information vital to the understanding and monitoring of disease that may lead to the design of better drug candidates for its treatment or prevention.

Specifically, this work demonstrates that nanoscale devices do, in fact, provide information that is not attainable with traditional macroscale devices. In terms of the LSPR nanosensor technology, several major accomplishments have been shown here. First, a successful sandwich assay for an antigen between two antibodies has been successfully demonstrated for the first time. This was accomplished, in part, because of our fundamental understanding and optimization of the spatial distribution of the electromagnetic fields surrounding the nanoparticles by controlling nanoparticle size and shape.[3,4] Next, without sacrificing the strength of nanoparticle adhesion to the substrate, the sensor's response exhibited no nonspecific binding in a pair of important assays. Quantitative binding models have been presented for both the detection of the target antigen and the second antibody in the antibody sandwich.

These models reveal important information regarding the nature of the ADDL targets as well as revealing two classes of binding affinity constants between the target antigens and antibodies. In contrast to our previous studies,[2,6] this binding model for direct ADDL detection does not perfectly fit the data (Figure 4A). At high concentrations, the response model accurately predicts the LSPR shift response; however, at low concentrations (that is, <10 pM ADDL), the response model underestimates the observed response. Because the LSPR shift response eventually goes to zero, the underestimation of the response cannot arise for nonspecific binding interactions. Instead, we hypothesize that this behavior reveals information regarding the nature of the endogenous ADDL molecules.

Surprisingly, this hypothesis is fully supported upon the analysis of the second anti-ADDL antibody shift response. This response can be divided into three ADDL concentration regions. In region 1 (1 fM to 10 pM), the ADDL molecules have an extremely high affinity ($K_{a,surf,1} = 7.3 \times 10^{12}$ M^{-1}) for the

antibody. From the quantitative model, which underestimates the LSPR response for ADDL detection in the sub-10 pM region, the actual response observed here suggests that the molecules have a higher molecular weight than the second class of ADDLs detected. This is apparent from the larger than predicted LSPR shifts observed in the direct ADDL response analysis. The results in region 2 (10 pM to 10 nM) verify this claim. The second class of molecules was revealed to have a binding constant, $K_{a,surf,2}$, about 9.5×10^8 M^{-1}. A comparison study using size exclusion chromatography (SEC) and ELISA revealed that ADDLs are comprised of two major types of molecules with different molecular weights (unpublished data). This is consistent with studies by Bitan and Teplow who detected different subpopulations in experiments with cross-linking reagents.[36] The data in region 3 (10 nM to 10 μM) reveals unusual behavior. The drop-off in the response was initially thought to arise from the so-called "Hook effect".[37,38] However, this type of behavior should be eliminated when a monoclonal antibody is used in place of the second polyclonal antibody. When this assay is repeated with a monoclonal second antibody, the hook effect is still observed (data not shown). Consequently, this response cannot be attributed to the Hook effect. Further work is in progress that seeks to understand this phenomenon. Our working hypothesis regarding this deviation is that at extremely high ADDL concentrations, small surface ADDLs (with a weak affinity to the first antibody) begin to interact and begin to behave as large ADDLs with higher binding affinities to the second antibody thereby being pulled off of the nanoparticles and exhibiting a reduction in second antibody response.

Finally, this work presents the first analysis of endogenous biological samples using LSPR detection. These extremely promising results indicate that the surface chemistry of the LSPR nanosensor has been designed for optimal analysis of complex biological species. The first set of samples discussed here confirms the previous observation that ADDLs are present in elevated concentrations in AD brain in comparison to a control.[34] Using the quantitative models, the magnitude of the shifts indicate that the ADDL concentration is ~1 pM in the diseased brain while the signal from the control sample is undetectable with the noise level (i.e., ~0). Again, the magnitude of the CSF shift indicates that a higher concentration of ADDLs or ADDL-related molecules is present in the CSF AD sample in comparison to the control. While the magnitude of the shift from the CSF sample is much larger than predicted by the ADDL response binding curve (Figure 4A), the second anti-ADDL antibody response indicates that the CSF sample contains ADDLs (possibly complexed to other molecules). This response is much larger than that observed in the analysis of the AD brain extract. At this time, we hypothesize that the oligomer size in CSF versus brain extract is quite different, perhaps influenced by the differing molecular milieus of CSF and brain extracts. Thus, it is most relevant to assess the two types of samples separately. Even though these studies must be regarded as preliminary given the small number of samples analyzed, they are, nonetheless, very exciting. They indicate that the LSPR nanobiosensor can be used to study human samples and may aid in the understanding of the mechanism and diagnosis of AD.

Conclusions

The success of this LSPR nanosensor was directly related to the synthesis and isolation of target biomolecules. By integrating this technology with the newly modified amyloid hypothesis, previously unavailable information has been revealed regarding the nature of ADDLs. All previous biophysical characterization of the oligomerization and fibrillogensis of these molecules typically required concentrations so high as to be irrelevant to in vivo conditions. The LSPR nanosensor has been demonstrated to be a powerful tool for studying the oligomerization of low concentrations of amyloid precursors. Given this success, the use of LSPR technology also holds promise as one of the best detection techniques for the screening of oligomerization-blocking drugs. Because the molecular causes and mechanisms of AD are not fully understood, devices that provide insight into the aggregated states of biological species and their interactions at native concentrations will help in screening patients for disease and possibly for studying drug interactions with target species. This work represents the first steps toward making this possible.

Acknowledgment. The authors gratefully acknowledge financial support from the Nanoscale Science and Engineering Initiative of the National Science Foundation under NSF Award EEC-0118025. Any opinions, findings, and conclusions or recommendations expressed in this material are those of the authors and do not necessarily reflect those of the National Science Foundation. W.L.K. gratefully acknowledges support from NIH. W.L.K. is co-founder of Acumen Pharmaceuticals, which has the sole license to patent rights owned by Northwestern University and the University of Southern California for use of ADDLs in the development of Alzheimer's-related therapeutics and diagnostics.

JA044087Q

(36) Bitan, G.; Kirkitadze, M. D.; Lomakin, A.; Vollers, S. S.; Benedek, G. B.; Teplow, D. B. *Proc. Natl. Acad. Sci. U.S.A.* **2003**, *100*, 330.
(37) Fernando, S. A.; Wilson, G. S. *J. Immunol. Methods* **1992**, *151*, 67.
(38) Fernando, S. A.; Wilson, G. S. *J. Immunol. Methods* **1992**, *151*, 47.